25th ABCM International Congress of Mechanical Engineering
October 20-25, 2019, Uberlândia, MG, Brazil

COB-2019-0772
INFLUENCE OF BIOMECHANICAL PARAMETERS ON THE GAIT IDENTIFICATION OF EXOSKELETON WITH UNSUPERVISED CLUSTERING ALGORITHM

Carlos Eduardo de Oliveira
Júlio César de Moraes Fernandes
Marcos Silveira
School of Engineering, São Paulo State University - UNESP, Bauru
ce.oliveira@unesp.br

Abstract. *The objective of this work is to study the kinematic behavior of an exoskeleton-like structure of lower limbs in order to identify gait patterns. Specifically, the influence of the length ratio between the tibia and the femur is shown, and the k-means unsupervised clustering algorithm is used to identify gait patterns using quantitative biomechanical metrics. The k-means algorithm was used with* 18 *metrics, variation of* R *and combinations of patterns of foot and pelvis. The results show that the k-means unsupervised algorithm was not able to correctly identify all four patterns when all 18 metrics were used. Further analysis showed that the use of fewer selected metrics can give very good identification. For example, when using only metrics* S_1 *and* A_C *it was possible to obtain 100% correct identification. In general, metrics* A_C*,* S_1*,* $\overline{x}_C$*,* x_{Cmax} *and* c_{min} *were the more successful in prediction of gait patterns.*

Keywords: *exoskeleton gait characterisation, biomechanical parameters, k-means clustering*

1. INTRODUCTION

Exoskeleton research has found applications in developing tools and equipment to aid human beings in daily activities, ranging from greater strength, endurance or agility, or for rehabilitation due to some trauma or disease (Chen *et al.*, 2016). Exoskeletons can be divided into two categories referring to the body part: upper limb and lower limb (Jardim, 2009). According to their purpose, they can be classified as assistive, intended to assist in the execution of lost function, and extensive, intended to increase the user's strength (Pons, 2008). Another application of exoskeletons is to help identify human gait patterns. Stancic *et al.* (2012) utilised kinematic parameters such as angular displacements and velocities related to the pelvis, ankle and knee for gait identification. A mechanical device was used to impose a limitation of the knee in order to simulate impairment. A gait patter factor comprised of a weighted sum of displacements, velocities and accelerations was introduced, enabling the identification in a more efficient manner than when using isolated kinematic parameters. Bittner *et al.* (2018) used a data driven approach to calculate the gradient of a cost function related to a large number of gait parameters. Among their contributions is a method to model local gait patterns from noisy measurements, which is common when using field data from robots and animals.

Yang *et al.* (2019) mentions some of the most recent technologies regarding robotics, among them are applications of exoskeletons. For example, Ding *et al.* (2018) shows a flexible exoskeleton adjustable to the user's body, which offers new ways of human integration similar to clothes. In this way it is possible to provide strength and balance without disturbing the natural movement of the user. The development of new actuators and force transducers is also important for the instrumentations of such exoskeletons. Kotikian *et al.* (2018) shows elastomeric actuators manufactured with high temperature 3D printing technology which are capable of exerting more force than other elastomeric actuators.

Considering this, the objective of this work is to study the kinematic behavior of an exoskeleton-like structure of lower limbs in order to identify gait patterns. Specifically, the influence of the length ratio between the tibia and the femur is shown, and the k-means unsupervised clustering algorithm is used to identify gait patterns using quantitative biomechanical metrics.

2. MATHEMATICAL EQUATIONS

The simplified exoskeleton model used in this study is shown in Fig. 1a, in which L_2 represents the lower leg and L_3 the upper leg. The trajectories of points B (foot) and D (pelvis) are assumed to be the ones described by Bezerra (2002), i.e. the foot can follow either a sinusoidal or elliptical trajectory, and the pelvis can folow either a sinusoidal or straight trajectory, as shown in Fig. 1b. For sinusoidal trajectory, the expressions of y_B and y_D are given by:

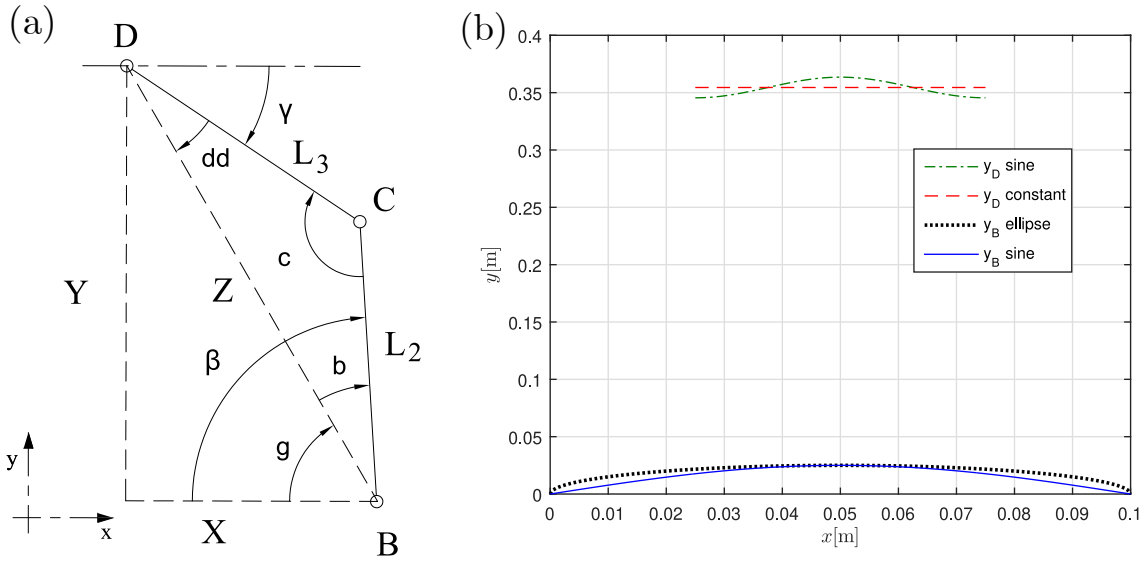

Figure 1. Simplified exoskeleton model with lower leg (L_2) and upper leg (L_3) and trajectory of B and D

$$y_B = A_B \sin((\omega_B x_B) + \phi_B) + a_{By} \qquad y_D = A_D \sin((\omega_D x_D) + \phi_D) + a_{Dy} \tag{1}$$

in which A_B and A_D are the amplitudes, ω_B and ω_D are the spatial frequencies, ϕ_B and ϕ_D are the phase angles, a_{By} is the distance from the ankle to the ground (which is set to zero) and a_{Dy} is the minimum distance from the pelvis to the ground. For elliptical trajectory of B, the expressions are given by:

$$y_B = A_B \sqrt{1 - \left(\frac{x_B^2}{r^2}\right)} + a_{By} \tag{2}$$

For the determination of coordinates of point C (knee), the distance Z and angles c, b, dd, g, β and γ are calculated according to:

$$\begin{aligned}
&X = x_B - x_D && Y = y_D - y_B && Z = \sqrt{X^2 + Y^2} \\
&c = \arccos\left(\frac{1}{2}\,\frac{Z^2 - L_3^2 - L_2^2}{L_3\, L_2}\right) && dd = \arccos\left(\frac{1}{2}\,\frac{L_2^2 - Z^2\, L_3^2}{Z\, L_3}\right) && b = \pi - c - dd \\
&g = \arccos\left(\frac{x_B - x_D}{Z}\right) && \gamma = b + g && \beta = g - dd
\end{aligned} \tag{3}$$

Once b and g are known, the coordinates of point C are given by:

$$\begin{aligned}
x_C &= x_B + L_2 \cos(\pi - g - b) \\
y_C &= y_B + L_2 \sin(\pi - g - b)
\end{aligned} \tag{4}$$

3. INFLUENCE OF BIOMECHANICAL PARAMETERS L_2 and L_3

The trajectories for a set of nominal parameters are shown for a combination of trajectories of B and D as follows: P_1 with B and D sinusoidal; P_2 with B sinusoidal and D straight; P_3 with B elliptical and D sinusoidal; P_4 with B elliptical and D straight. These trajectories are shown in Fig.1b. The parameters used are as follows: $tp = 0.100$ m, $L_3 = 0.18182$ m, $L_2 = 0.18182$ m, $t_d = 0.050$ m, $A_D = 0.009$ m, $a_{Dy} = 0.3995$ m, $a_{Dx} = 0.0255$ m, $A_B = 0.025$ m, $a_{By} = 0.0495$ m, $A_D = 0.009$ m. Based on the nominal values, the values of L_2 and L_3 are varied from 0.14330 to 0.23883 m. Consequently, the ratio $R = L_3/L_2$ varies from 0.6 to 1.667. Figures 2 and 3 show the trajectory of C, as well as the displacements and angles as function of x_B for these nominal parameters for combinations P_1 and P_2, respectively.

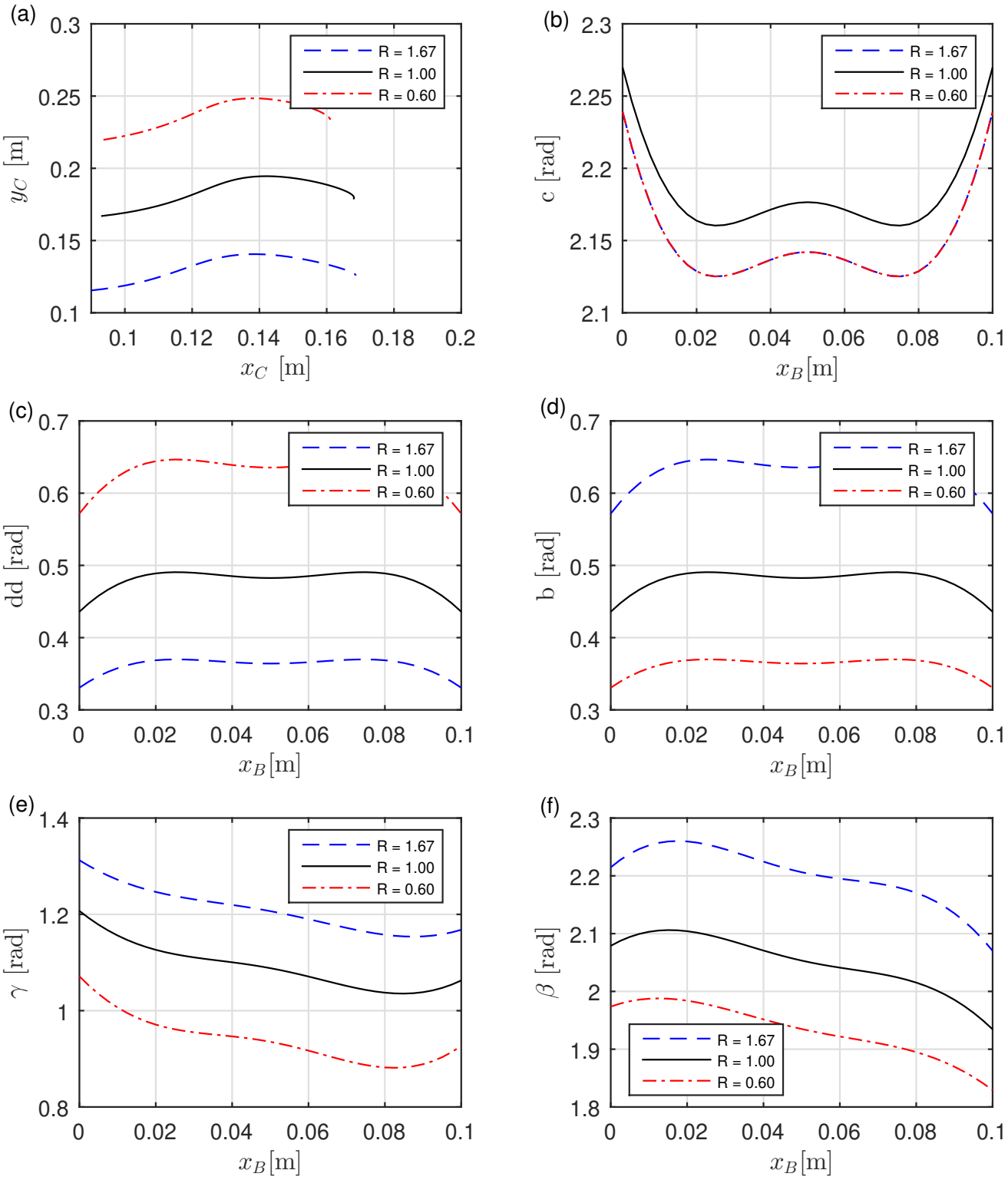

Figure 2. Trajectory of C and the behaviour of c, dd, b, β, γ as function of x_B for pattern P_1

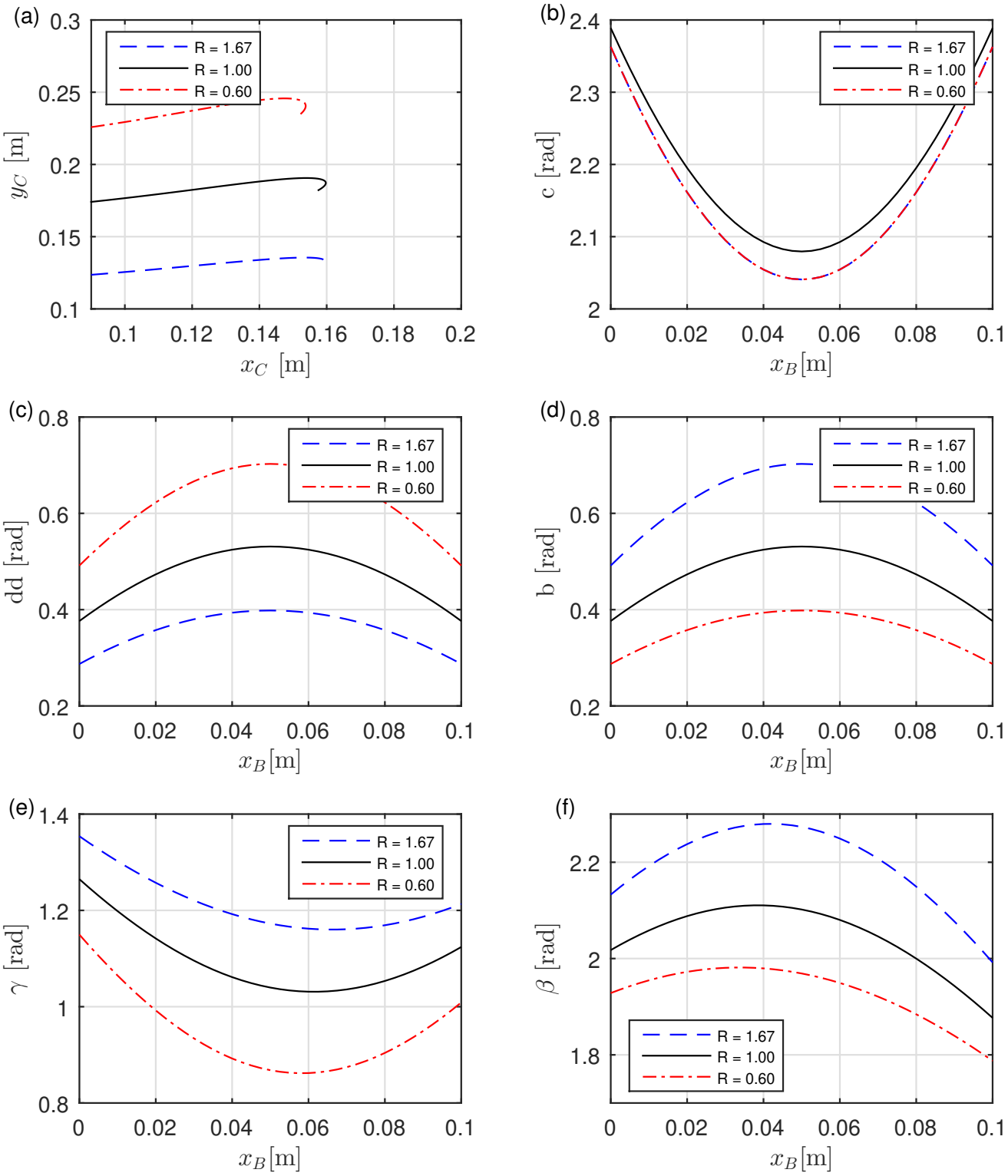

Figure 3. Trajectory of C and the behaviour of c, dd, b, β, γ as function of x_B for pattern P_2

4. METRICS USED FOR CLUSTERING

In order to use the clustering algorithm, the following metrics related to the trajectories from Figs. 2 and 3 are defined: area (A_C), arc length from maximum to minimum points $(S1)$, arc length from maximum to final points $(S2)$, arc length from initial to final points $(S3)$, maximum point, minimum point, amplitude, mean. The area, arc length and mean are used for trajectories of the knee, maximum values are used for angles dd, b and beta, minimum values are used for angles c and gamma, the amplitude is used for the knee trajectory and knee angle. Table 1 summarises all the metrics used with respective symbols, and Eq. (6) defines these metrics.

$$A_c = \int_{x_{in}}^{x_{fin}} C(x_C, y_C)dx \qquad S = \sum \sqrt{\Delta {x_C}^2 + \Delta {y_C}^2} \qquad \Delta_y = y_{max} - y_{min}$$
$$\overline{y} = \frac{\sum y}{N} \qquad \Delta_x = x_{max} - x_{min} \qquad \overline{x} = \frac{\sum x}{N} \tag{5}$$

in which N is the number of points in the trajectories.

Table 1. Biomechanical Metrics

Symbol	Metric
(A_C)	Area of C trajectory
(S_1)	Arc length (initial to final point)
(S_2)	Arc length (maximum to final point)
(S_3)	Arc length (initial point to maximum)
(y_{Cmax})	Maximum y_C
(dd_{max})	Maximum dd
(b_{max})	Maximum b
(β_{max})	Maximum β
(x_{Cmax})	Maximum x_C
(c_{min})	Minimum c
(γ_{min})	Minimum γ
(Δy)	Amplitude of y
(Δx)	Amplitude of x
$(\overline{y}_C)$	Mean y_C
$(\overline{c})$	Mean c
$(\overline{\gamma})$	Mean γ
$(\overline{\beta})$	Mean β
$(\overline{x}_C)$	Mean x_C

5. RESULTS OF k-MEANS UNSUPERVISED CLUSTERING

The 18 metrics listed in Table 1 were organised in matrix form, as follows:

$$A = [A_C\ S_1 S_2\ S_3\ y_{Cmax}\ dd_{max}\ b_{max}\ \beta_{max}\ x_{Cmax}\ c_{min}\gamma_{min}\ \Delta_y\ \Delta_x\ \overline{y}_C\ \overline{c}\ \overline{\gamma}\ \overline{\beta}\ \overline{x}_C] \tag{6}$$

Each line corresponding to values obtained from combination of the 21 values of R and 4 patterns P, giving a totla of 84 lines. After assembly, each column was normalised to be used as input data for the k-means algorithm. The number of clusters was set to 4, and the Squared Euclidean distance was used to calculate the centroid.

Figures 4–6 show the results of the k-means with all 18 metrics, displayed as projections in some 2D planes opf interest. For each plane, k-means was applied again, but only to the 2 metrics relative to each projection, with the objective of showing the influence of this trajectories on the clustering performance to identify patterns $P_1 - P_4$.

Figure 4a shows that k-means is not able to identify the patterns correctly when all 18 metrics are used, and Fig. 4b shows that the identification is successful using only S_1 and A_C as inputs. Figure 4d shows that using only x_{Cmax} and x_C has a better result than all metrics together, correctly identifying P_1, although other points are mislabelled. Figure 4f shows that metric c_{min} and γ_{min} do not provide good identification.

Figures 5a and 5b shows that using S_1 and c_{min} it is possible to identify P_1 and P_2, although the other 2 clusters have mislabelled points. Figures 5c and 5d show that S_2 and β_{max} are not good predictors for patterns. However, it is possible to see that it distinguishes well between P_1–P_2 (B sinusoidal) and P_3–P_4 (B elliptical). Figures 5e and 5f show similar behaviour for y_{Cmax} and A_C: identification is not correct, it distinguishes well between P_1–P_3 (D sinusoidal) and P_2–P_4 (D straight).

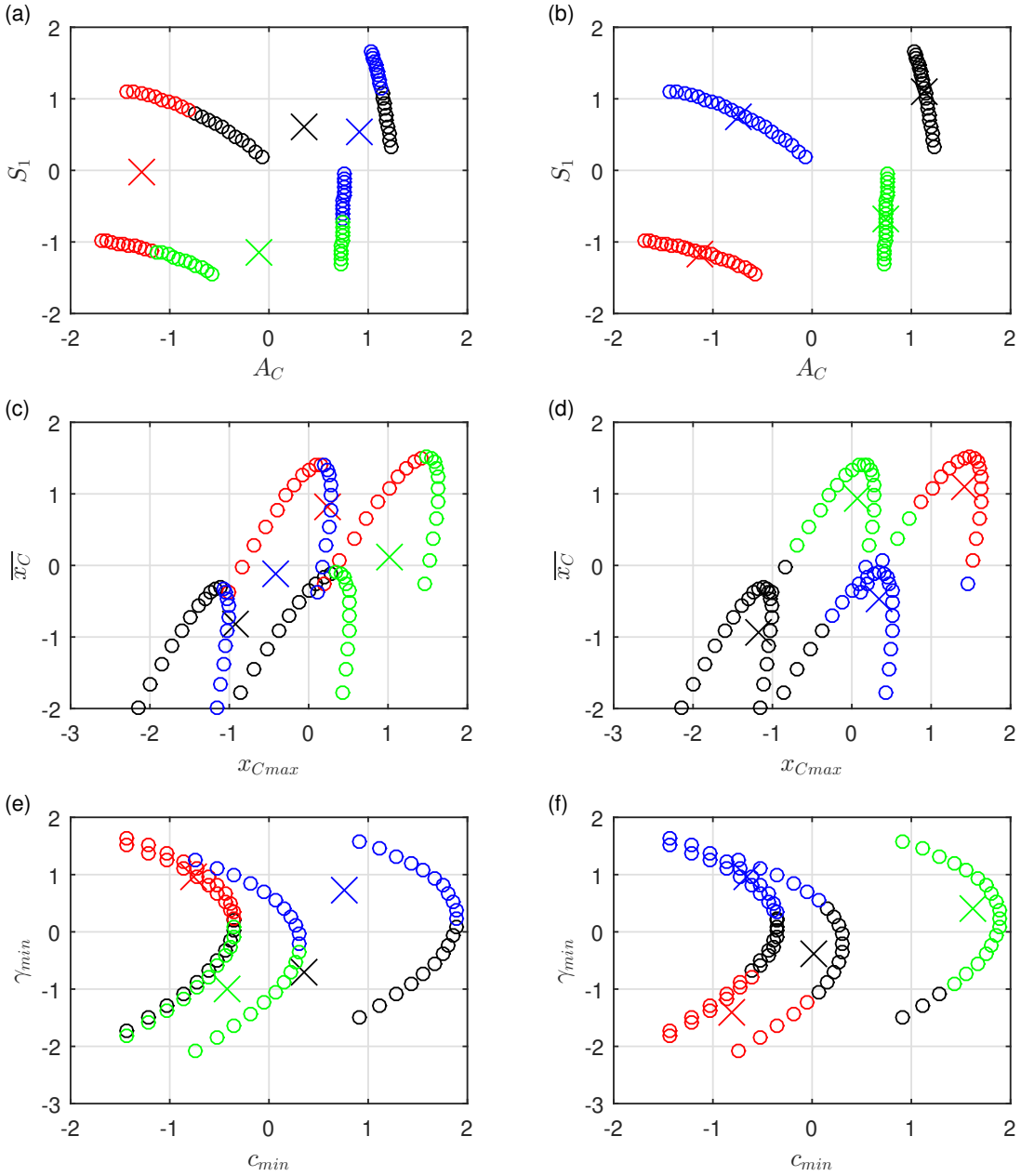

Figure 4. Results *k-means* with $k = 4$ applied to array A

Figures 6a and 6b show results for A_C and c_min, showing good identification of P_1 and P_3, although mislabelled points appear. Figures 6c and 6d show that S_1 and C_{max} give good identification of P_2 and P_4, with few mislabelled points.

6. CONCLUSIONS

This work presented the kinematic equations of a simplified lower limb assistive exoskeleton model allowing variation of the biomechanical parameters. With the results from the numerical simulations, it is possible to identify the behaviour of the ankle, knee and pelvis angles, as well as trajectory of the knee, showing that the ratio of upper leg and lower leg sizes (R) has relevant influence.

The *k-means* algorithm was used with 18 metrics, variation of R and combinations of patterns of foot and pelvis. The results show that the k-means unsupervised algorithm was not able to correctly identify all four patterns when all 18 metrics were used. Further analysis showed that the use of fewer selected metrics can give very good identification. For example, when using only metrics S_1 and A_C it was possible to obtain 100% correct identification. In general, metrics A_C, S_1, $\overline{x}_C$, x_{Cmax} and c_{min} were the more successful in prediction of gait patterns.

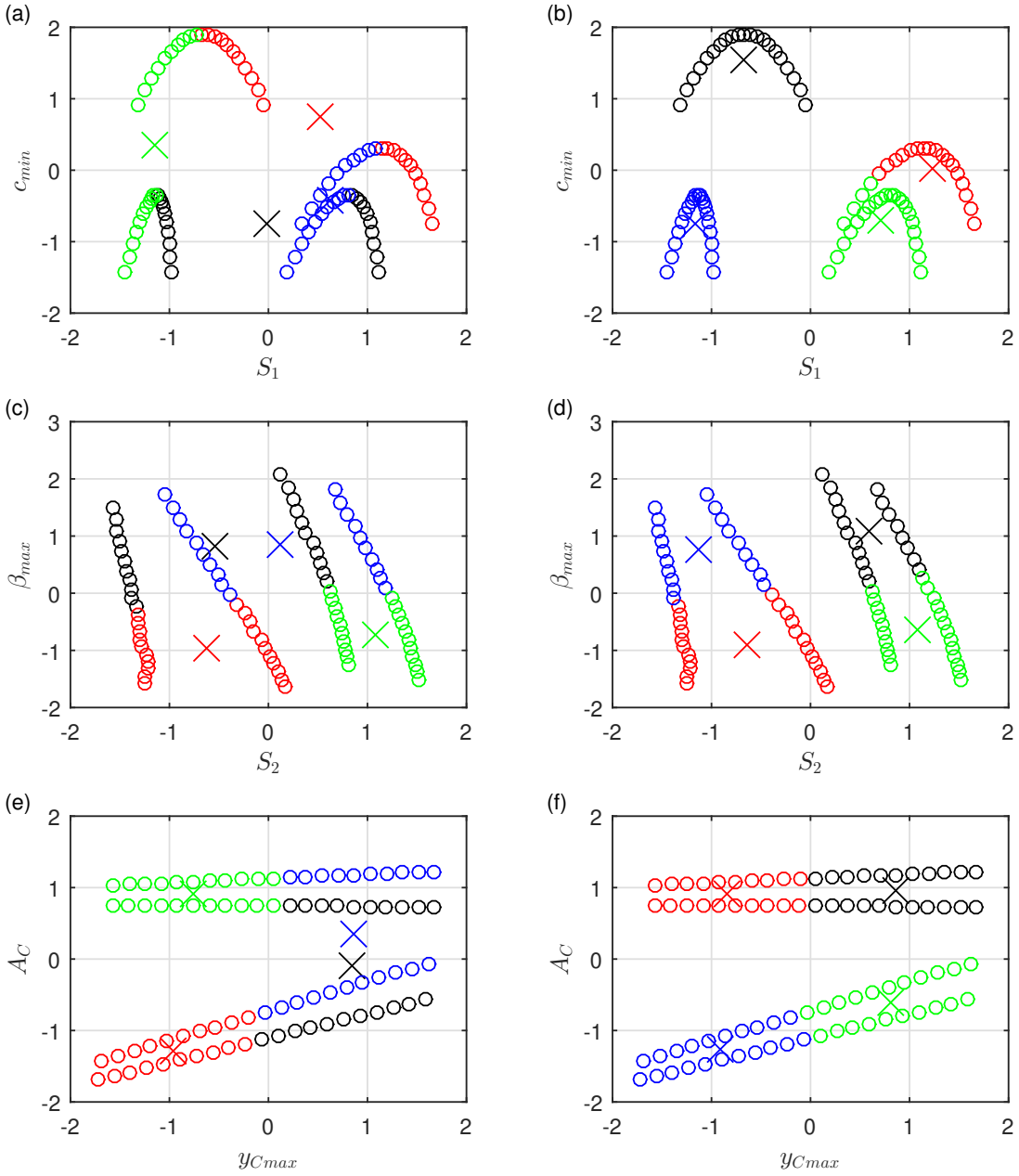

Figure 5. Results *k-means* with $k = 4$ applied to array A

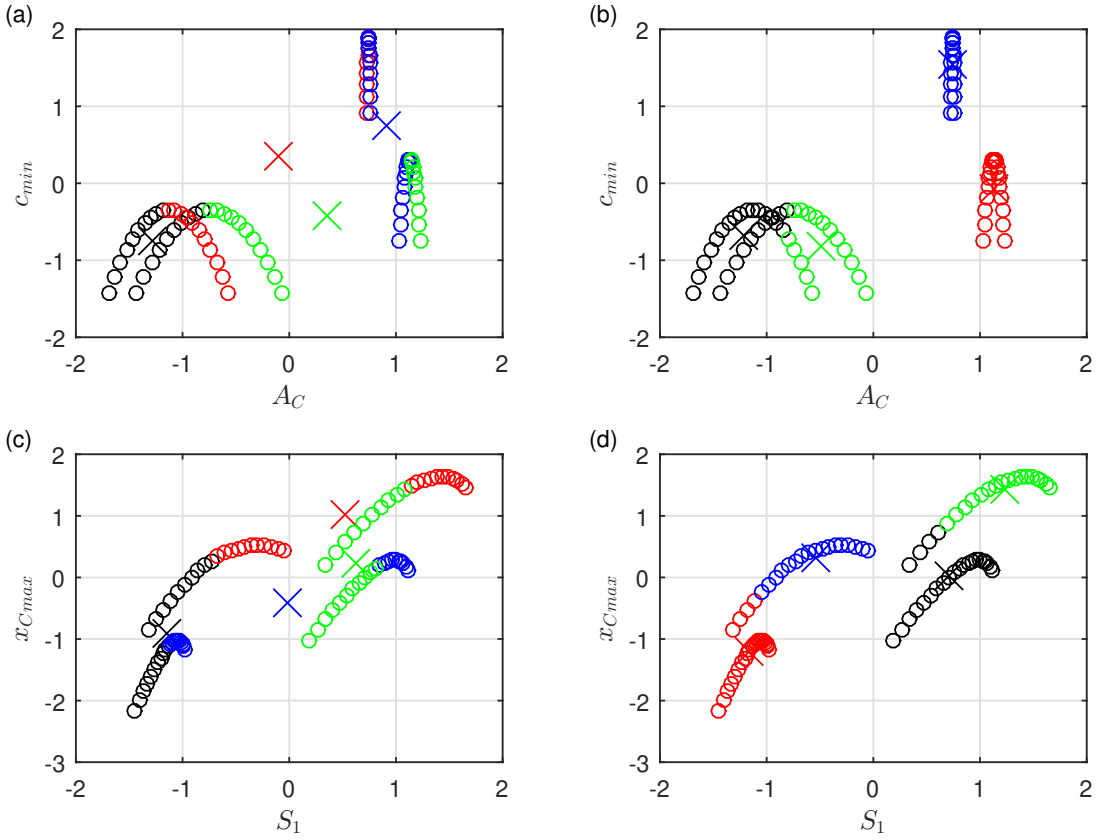

Figure 6. Results *k-means* with $k = 4$ applied to array A

7. ACKNOWLEDGEMENTS

The authors thank the research group.

8. REFERENCES

Bezerra, C.A.D., 2002. *Desenvolvimento de um robo bipede para locomoção em ambiente desestruturado*. Ph.D. thesis, Universidade Estadual de Campinas.

Bittner, B., Hatton, R.L. and Revzen, S., 2018. "Geometrically optimal gaits: a data-driven approach". *Nonlinear Dynamics*, Vol. 94, No. 3, pp. 1933–1948.

Chen, B., Ma, H., Qin, L.Y., Gao, F., Chan, K.M., Law, S.W., Qin, L. and Liao, W.H., 2016. "Recent developments and challenges of lower extremity exoskeletons". *Journal of Orthopaedic Translation*, Vol. 5, pp. 26–37.

Ding, Y., Kim, M., Kuindersma, S. and Walsh, C.J., 2018. "Human-in-the-loop optimization of hip assistance with a soft exosuit during walking". *Sci. Robot.*, Vol. 3, No. 15, p. eaar5438.

Jardim, B., 2009. *Atuadores Elásticos em Série Aplicados no Desenvolvimento de um Exoesqueleto para Membros Inferiores. 2009. 102f.* Master's thesis, Escola de Engenharia de São Carlos, Universidade de São Carlos, São Carlos.

Kotikian, A., Truby, R.L., Boley, J.W., White, T.J. and Lewis, J.A., 2018. "3d printing of liquid crystal elastomeric actuators with spatially programed nematic order". *Advanced Materials*, Vol. 30, No. 10, p. 1706164.

Pons, J.L., 2008. *Wearable robots: biomechatronic exoskeletons*. John Wiley & Sons.

Stancic, I., Supuk, T.G. and Bonkovic, M., 2012. "New kinematic parameters for quantifying irregularities in the human and humanoid robot gait". *International journal of advanced robotic systems*, Vol. 9, No. 5, p. 215.

Yang, G.Z., Full, R.J., Jacobstein, N., Fischer, P., Bellingham, J., Choset, H., Christensen, H., Dario, P., Nelson, B.J. and Taylor, R., 2019. "Ten robotics technologies of the year".

9. RESPONSIBILITY NOTICE

The authors are the only responsible for the printed material included in this paper.